Solid State Ionics 292 (2016) 83–87

Contents lists available at ScienceDirect

Solid State Ionics

journal homepage: www.elsevier.com/locate/ssi

# Structural features and high-temperature properties of $SrFe_{1-x}Si_xO_{3-\delta}$

O.V. Merkulov [a,*], A.A. Markov [a], M.V. Patrakeev [a], A.V. Chukin [b], I.A. Leonidov [a], V.L. Kozhevnikov [a]

[a] Institute of Solid State Chemistry, UB RAS, 91 Pervomayskaya Str., 620990 Yekaterinburg, Russia
[b] Ural Federal University, 19 Mira Str., 620002 Yekaterinburg, Russia

ARTICLE INFO

*Article history:*
Received 28 January 2016
Received in revised form 26 April 2016
Accepted 7 May 2016
Available online 3 June 2016

*Keywords:*
Si-substituted strontium ferrite
Perovskite
Thermal expansion
Mixed conductivity
Oxygen vacancies, phase stability

ABSTRACT

The perovskite-like oxide series $SrFe_{1-x}Si_xO_{3-\delta}$, where $x = 0.05, 0.10, 0.15, 0.20, 0.25$ and $0.30$, was obtained by the solid state synthesis at 1300 °C. The maximal solubility of silicon is found to be near $x_m = 0.25$. The observed increase of the cubic lattice parameter with silicon content is shown to be mainly related with reduction of iron cations. The silicon doping is also accompanied with the decrease of oxygen homogeneous range and expansion of $SrFe_{1-x}Si_xO_{3-\delta}$ ceramics at heating in air. It is shown that silicon dopants influence rather weakly the electron–hole contribution to the total conductivity while oxygen ion component undergoes a strong decline. The dependence of the ion conductivity from silicon content can satisfactorily be explained in frameworks of the model with oxygen vacancies trapped near silicon dopants.



## 1. Introduction

Perovskite-like strontium ferrite $SrFeO_{3-\delta}$ is a promising oxide that can be useful in high-temperature applications such as oxygen separation and storage, sensors and SOFCs owing to its good robustness at changes of oxygen pressure and temperature, high level of both electron and oxygen ion conductivity components, and exceptionally large range of homogeneous oxygen content, $0 \le \delta \le 0.5$ [1–8]. However, the tendency of oxygen vacancies to ordering can deleteriously affect structural stability and conductivity, particularly in the limit $\delta \to 0.5$ where $SrFeO_{3-\delta}$ undergoes a cubic to orthorhombic structure phase transformation at temperatures below 870 °C [6,9–12]. The transition can be prevented by partial replacement of iron by titanium, chromium, gallium or aluminum cations [13–19]. It is believed that the observed retention of the cubic perovskite crystalline framework is related with suppression of oxygen vacancy ordering at random distribution of doping cations [13,15–17].

Another approach was proposed recently for modification of $SrFeO_{3-\delta}$ based materials and stabilization of the cubic structure through incorporation of silicate oxyanions $(SiO_4)^{4-}$ [20,21]. The obtained materials showed improved conductivity and decreased area specific resistance. However, measurements were carried out only in air and 5% $H_2$/95% $N_2$ atmospheres and a number of issues remain unresolved. Particularly, it is important to evaluate ion conductivity in $SrFe_{1-x}Si_xO_{3-\delta}$, thermal expansion and stability of materials under reducing conditions.

In this work we present the data on synthesis, thermal expansion and high-temperature conductivity of $SrFe_{1-x}Si_xO_{3-\delta}$ at wide variations of oxygen partial pressure. The results are used in order to obtain oxygen ion and electron contributions, and to evaluate stability of the materials at low pressures of oxygen.

## 2. Experimental

High-purity reagents SrCO3 (99.9%), $Fe_2O_3$ (99.2%) and $SiO_2$ (99.5%) were used for solid state synthesis of $SrFe_{1-x}Si_xO_{3-\delta}$, where $x = 0.05$, 0.10, 0.15, 0.20, 0.25 and 0.30. The starting materials were calcined at 400–450 °C in order to remove adsorbates, weighed in desirable proportions, thoroughly ground with a mortar and pestle and fired at 1000 °C in air for 10 h. After that the samples were reground and heated at 1100 °C for further 10 h. The procedure was repeated with heating at 1200 and 1300 °C. The obtained powder materials were pelletized at 200–300 MPa of uniaxial pressure and fired in air again for 10 h at 1300 °C. The resulting ceramic pellets were partially pulverized for further thermogravimetric and X-ray diffraction measurements. Also, rectangular $2 \times 2 \times 12$ and $2 \times 2 \times 4$ mm bars were cut from the pellets for electrical conductivity and thermal expansion measurements, respectively. Moreover, some part of the prepared samples was treated for 24 h at 950 °C in the stream of a gas mixture 89% Ar/10% $CO_2$/1% CO where oxygen activity was near $10^{-12}$ atm. Then the samples were cooled down to room temperature with the rate of 5 °C/min in the same gas flow.

Powder X-ray diffraction (XRD) in Bragg–Brentano mode was used for phase purity control and determination of crystal lattice parameters in the obtained samples. The diffraction patterns were collected at room temperature with the help of a PANalytical X'pert Pro diffractometer

* Corresponding author.
*E-mail address:* merkulov@ihim.uran.ru (O.V. Merkulov).

http://dx.doi.org/10.1016/j.ssi.2016.05.014
0167-2738/

using CuKα-radiation. The structural parameters were calculated employing PCW 2.4 software [22].

The variations of oxygen content in $SrFe_{1-x}Si_xO_{3-\delta}$ with temperature were studied in air with the use of a Setaram TG-92 thermoanalyzer at heating/cooling rate of 1 °C/min. Thermal expansion measurements in air were carried out with the help of a Linseis L75 dilatometer at heating rate of 5 °C/min.

The electrical dc conductivity was measured in a special tubular cell made of cubically stabilized zirconia (YZS) oxygen electrolyte. Two pairs of platinum electrodes were deposited on inner and outer sides of the cell and served as oxygen electrochemical pump and the sensor. The cell was heated with an external co-axial electric furnace, and enabled independent setting and control of the oxygen partial pressure ($p_{O_2}$) around the specimen via computer control of the pump and sensor. Potential probes and current leads for four-probe conductivity measurements were made of Ø 0.3 mm Pt wire and tightly wound on the sample with an 6- and 10- mm spacing, respectively. The specimen was set perpendicular to the cell axis and maintained in the isothermal conditions with a special holder. The cell with the wired specimen was evacuated and filled with the gas mixture containing 50% $O_2$ and 50% $CO_2$ in the beginning of the measurements. The conductivity data were collected at 700–950 °C with the temperature step 50 °C in the oxygen partial pressure (activity) range $10^{-20}$–0.5 atm. The measurements were carried out in the mode of step-like decreasing oxygen partial pressure in isothermal runs. When the lower pressure limit was achieved the pressure was increased to the upper limit, and the measurements were repeated in order to confirm reversibility of the experiment and reproducibility of the data. The temperature was then changed and the measuring cycle recurred. The relaxation time after a change in the oxygen pressure over a sample varied from 20 min to several hours and was dependent on the temperature and oxygen partial pressure range. The criterion for achieving equilibrium was accepted as a relaxation rate of less than 0.1% per minute in the logarithm of the conductivity under a fixed oxygen pressure inside the cell. The electrical parameters were measured with a high-precision voltmeter Solartron 7081. More experimental details can be found elsewhere [23,24].

## 3. Results and discussion

### 3.1. Structure, thermal expansion and oxygen content variations

Powder XRD patterns of the obtained samples $SrFe_{1-x}Si_xO_{3-\delta}$, where $x = 0.05, 0.10, 0.15, 0.20, 0.25$ and $0.30$, are shown in Fig. 1. In difference with the pristine tetragonal ferrite $SrFeO_{3-\delta}$ [9], the silicon substituted specimens show formation of a single cubic perovskite-like phase (S.G. $Pm\bar{3}m$) up to $x = 0.25$. Further increase of silicon content to $x = 0.30$ results in appearance of weak reflections of strontium orthosilicate $Sr_2SiO_4$ (S.G. *Pnmb*). The refinement of the spectrum with a two-phase model shows that the specimen with the nominal composition $SrFe_{0.7}Si_{0.3}O_{3-\delta}$ may contain about 4 vol. % of $Sr_2SiO_4$ with the unit cell parameters $a = 5.664(9)$ Å, $b = 7.065(5)$ Å and $c = 9.723(0)$ Å, while the main phase component is the cubic perovskite with the lattice parameter $a = 3.902(0)$ Å. This value coincides with that one in $SrFe_{0.75}Si_{0.25}O_{3-\delta}$ within experimental uncertainties, Fig. 2. Interestingly, no iron rich impurities were detected in $SrFe_{0.7}Si_{0.3}O_{3-\delta}$. One can suppose, therefore, that appearance of a small amount of $Sr_2SiO_4$ was charge compensated by formation of strontium vacancies in the main phase $SrFe_{0.75}Si_{0.25}O_{3-\delta}$, which borders the solid solution $SrFe_{1-x}Si_xO_{3-\delta}$. In fact, perovskite-like ferrites are known to endure at least 3% deficiency in A-sublattice [25]. Therefore, one can conclude that the maximum solubility of silicon in $SrFe_{1-x}Si_xO_{3-\delta}$ is $x_m = 0.25$. This is larger than $x_m = 0.15$ in work [20]. However, the observed difference can be explained as a consequence of the higher synthesis temperature used in the present study.

It is interesting to notice that $x_m = 0.25$ is consistent with the structural features of strontium ferrite. Actually, the air synthesized $SrFeO_{3-\delta}$ is characterized with $\delta = 0.125$ [26]. The appearance of oxygen vacancies is accompanied with partial reduction of $Fe^{4+}$ to $Fe^{3+}$ cations and transformation of iron-oxygen octahedra ($FeO_{6/2}$) to square pyramids ($FeO_{5/2}$) that have smaller size compared to octahedra. Accordingly, the crystallochemical formula of the ferrite with $\delta = 0.125$ can be presented as $Sr(FeO_{6/2})_{0.75}(FeO_{5/2})_{0.25}$ [9,26]. One may expect from this formula that small silicate oxyanions must preferentially replace relatively small iron-oxygen pyramids and promote further reduction of $Fe^{4+}$ cations. Another interesting feature is the linear increase of the lattice parameter with silicon content in $SrFe_{1-x}Si_xO_{3-\delta}$, Fig. 2. On the one hand, silicon incorporation in the ferrite structure is accompanied with removal of oxygen from the crystalline lattice [21] and reduction of $Fe^{4+}$ ($R_{CN6} = 0.585$ Å) to larger $Fe^{3+}$ ($R_{CN6} = 0.645$ Å) cations [27], and, indeed, this change is favorable for the increase of the lattice parameter. On the other hand, replacement of iron by much smaller $Si^{4+}$ cations ($R_{CN4} = 0.260$ Å) may facilitate a decrease in the lattice parameter. Therefore, the observed net increase of the lattice parameter is governed mainly by reduction of iron cations while structural distortions localized near $SiO_4$ tetrahedra do not influence substantially the unit cell volume in the air-synthesized samples $SrFe_{1-x}Si_xO_{3-\delta}$.

The XRD patterns for $SrFe_{1-x}Si_xO_{3-\delta}$ after reducing treatment at 950 °C and $p_{O_2} = 10^{-12}$ atm are shown in Fig. 3. The most obvious changes have taken place in the diffraction pattern for the sample with $x = 0.05$ where in addition to perovskite-like $Sr(Fe,Si)O_{3-\delta}$ ($Pm\bar{3}m$) reflections of brownmillerite-like $Sr_2(Fe,Si)_2O_5$ (S.G. *Ibm2*) phase can be observed. The use of a two-phase model at fitting of the diffraction data results in 23 and 77 vol. % of *Ibm2* and $Pm\bar{3}m$ phases,

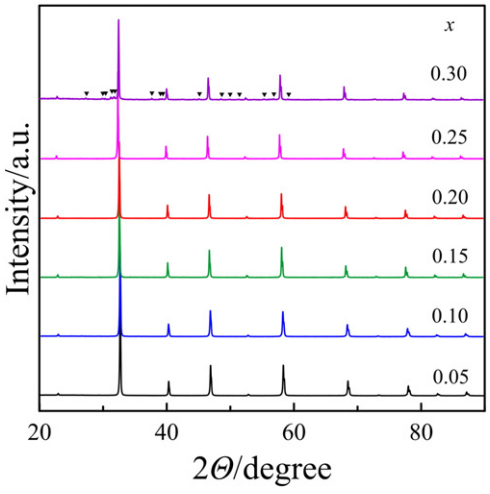


**Fig. 1.** X-ray powder diffraction patterns for air-prepared $SrFe_{1-x}Si_xO_{3-\delta}$. The triangles show reflections of $Sr_2SiO_4$.

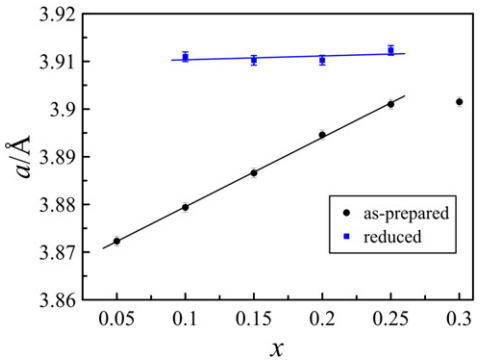


**Fig. 2.** The changes of the unit cell parameter in $SrFe_{1-x}Si_xO_{3-\delta}$ with silicon content.